ACS Partner Journal

Journal of the American Society for Mass Spectrometry

pubs.acs.org/jasms

Research Article

# Localization of Intrachain Modifications in Bacterial Lipids Via Radical-Directed Dissociation

Qiaohong Lin, Pengyun Li, Ruijun Jian, and Yu Xia*

Cite This: *J. Am. Soc. Mass Spectrom.* 2022, 33, 714−721

Read Online

ACCESS | Metrics & More | Article Recommendations | Supporting Information



**ABSTRACT:** Intrachain modifications of membrane glycerophospholipids (GPLs) due to formation of the carbon−carbon double bond (C═C), cyclopropane ring, and methyl branching are crucial for bacterial membrane homeostasis. Conventional collision-induced dissociation (CID) of even-electron ions of GPL favors charge-directed fragmentation channels, and thus little structurally informative fragments can be detected for locating intrachain modifications. In this study, we report a radical-directed dissociation (RDD) approach for characterization of the intrachain modifications within phosphoethanolamines (PEs), a major lipid component in bacterial membrane. In this method, a radical precursor that can produce benzyl or pyridine methyl radical upon low-energy CID at high efficiency is conjugated onto the amine group of PEs. The carbon-centered radical ions subsequently initiate RDD along the fatty acyl chain, producing fragment patterns key to the assignment and localization of intrachain modifications including C═C, cyclopropane rings, and methyl branching. Besides intrachain fragmentation, RDD on the glycerol backbone produces fatty acyl loss as radicals, allowing one to identify the fatty acyl chain composition of PE. Moreover, RDD of lyso-PEs produces radical losses for distinguishing the *sn*-isomers. The above RDD approach has been incorporated onto a liquid chromatography−mass spectrometry workflow and applied for the analysis of lipid extracts from *Escherichia coli* and *Bacillus subtilis*.

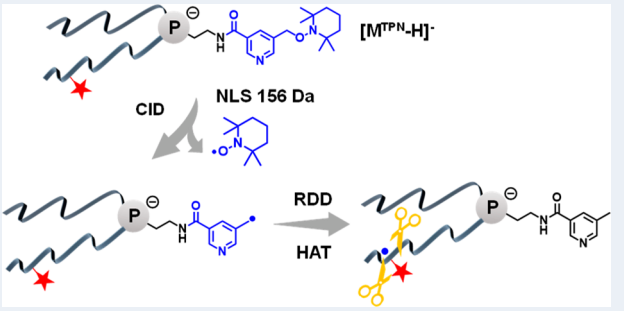


**KEYWORDS:** *tandem mass spectrometry, radical-directed dissociation, lipidomics, methyl branching, cyclopropane*

## INTRODUCTION

Bacteria adjust membrane lipid structures and compositions to survive and prosper in a wide variety of environmental conditions. One of the mechanisms for modifying a lipid structure is to initiate intrachain modifications within membrane glycerophospholipids (GPLs). The common ones include forming the carbon−carbon double bond (C═C), cyclopropane ring, and methyl branching.[1,2] The introduction of *cis*-C═C rather than *trans*-C═C in GPLs leads to lower transition temperatures and higher permeability of membranes.[1] Besides unsaturation, bacteria such as *Escherichia coli* and *Mycobacterium tuberculosis* utilize cyclopropane modification to enhance membrane fluidity and construct more stable membranes against hostile environments.[3] Cyclopropane modification is assisted by cyclopropane fatty acid synthase (Cfa) and formed via the addition of a methylene group across the C═C bonds of unsaturated fatty acyls of GPLs.[4,5] Methyl branching is a high-frequency modification found in Gram-positive bacteria such as *Staphylococcus aureus* and *Bacillus subtilis* and, to a lesser extent, in mammals.[6−8] Methyl branching typically happens at the penultimate (*iso*) or antepenultimate (*anteiso*) carbons. Their biosynthetic pathways involve the incorporation of valine, leucine, and isoleucine.[9] The above-mentioned intrachain modifications are found to be associated with pH and temperature adaptation.[2,10] Therefore, characterizing these modifications is increasingly important for the understanding of their functions in biomembranes.

Advances in electrospray ionization tandem mass spectrometry (ESI-MS/MS) have made it a preeminent technology for a fast and sensitive lipid analysis.[11,12] Conventional lipidomics profiling protocols relying on low-energy collision-induced dissociation (CID) readily provide critical structural information regarding the lipid class and identities of the fatty acyls, that is, the length and degree of unsaturation of individual fatty acyls in lipids.[13,14] However, detailed information on the modifications on acyl chains, such as the site(s) of C═C, cyclopropane, and methyl branching, is difficult to gain due to the lack of structurally informative fragments formed in low-energy CID.

**Received:** January 15, 2022
**Revised:** February 17, 2022
**Accepted:** February 17, 2022
**Published:** February 23, 2022

**Scheme 1. Major RDD Pathways Initiated by CID of TPN-Derivatized PE: Intrachain Fragmentation and Fatty Acyl Fragmentation**

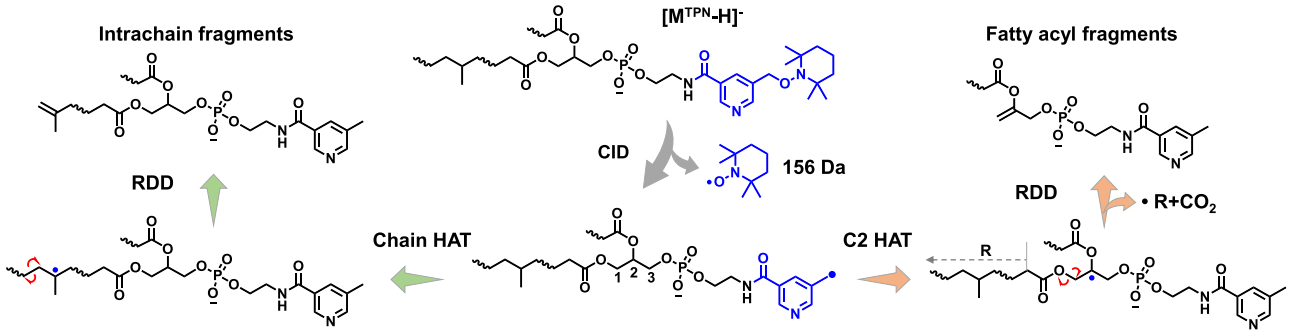


To address this challenge, several alternative MS/MS methods have been developed to provide access to deeper levels of structural elucidation for lipids. One of the strategies for pinpointing the C=C location in unsaturated fatty acyls involves a specific derivatization of the C=C into a functional group that is prone to CID. These derivatizations include the Paternò-Büchi (PB) reaction,[15,16] epoxidation,[17,18] and singlet oxygen-ene reaction.[19] Gas-phase ion activation methods, such as ozone-induced dissociation (OzID),[20,21] electron impact excitation of ions from organics (EIEIO),[22] ultraviolet photodissociation (UVPD),[23,24] have also been explored to assign sites of unsaturation. For cyclopropane modification, the Brodbelt group demonstrated 213 nm UVPD for its characterization in bacterial lipids based on cross-ring C−C cleavages of the cyclopropane ring.[25] The McLuckey group employed charge inversion ion/ion reactions for the characterization of cyclopropane motifs in cardiolipin fatty acyls from *E. coli* lipid extracts.[26]

Radical-directed dissociation (RDD) can introduce intrachain fragmentation, thus allowing localizing C=C, cyclopropane, hydroxy group, and methyl branching in fatty acyls. Because the lipid radical ions typically are not directly formed via ESI, lipid ions that are derivatized or complexed with a structure containing a C−I bond are formed by ESI first, and then the radical ions are uncaged after homolytic cleavage of the C−I bond upon 266 nm UVPD.[27−31] Alternatively, our group showed that the CID of the bicarbonate anion adducts of lipids containing a choline functional group produced a carbon-centered radical from the homolytic cleavage of the C−N bond in the ethylamine motif of the headgroup.[32] This further triggered minor RDD in the fatty acyls, permitting the assignment of locations of C=C and the discrimination of *iso*- and *anteiso*-methyl branching in lyso-phosphocholines (LPCs)[33] and sphingomyelins (SMs).[34] The above method, however, cannot be directly applied to phosphoethanolamines (PEs), which is one of the main lipid components of bacterial membrane.

In this study, we are motivated to develop an RDD method that produces lipid radical ions at high efficiency via CID and explore its potential in characterizing intrachain modifications for PEs in bacterial lipidome. Inspired by the free radical-initiated peptide sequencing (FRIPS),[35,36] a radical precursor that can release a benzyl radical or pyridine methyl radical upon CID is conjugated onto the amine functional group of lipids. The uncaged lipid radical ions subsequently initiate RDD within the fatty acyls as well as glycerol backbone via a hydrogen atom transfer (HAT), leading to intrachain fragments and fatty acyl fragments (Scheme 1). We demonstrate the capability of the above RDD method in defining the site of unsaturation, cyclopropane modification, and methyl branching in PEs and lyso-PEs (LPEs) as well as identifying the *sn*-isomers of LPEs from lipid extracts of bacteria.

## EXPERIMENTAL SECTION

**Lipid Nomenclature.** The shorthand notations for GPLs updated by Liebisch et al.[37] is adopted wherever possible. For instance, in PE 16:0/18:1, the forward slash "/" means known *sn*-positions of the two fatty acyls on the glycerol backbone, while an underscore separator "_" suggests unspecified *sn*-positions. The fatty acyl chain is denoted as the number of C atoms: the number of double bonds as in PE 16:0/18:1. The location of a C=C, however, is defined by *n*-x nomenclature, counting from the methyl end of the fatty acyl ester, followed by an annotation of C=C geometry (*Z* or *E*) if known. For fatty acyls containing cyclopropane, they are described with the *n*-x position for the ring, followed by a letter "c", as in C17:1(*cn*-7). Methyl branching at the penultimate carbon (*n*-2) or antepenultimate carbon (*n*-3) is indicated by "iso-" (abbreviated as "i") or "anteiso-" (abbreviated as "a"), respectively.

**Chemicals and Materials.** Lipid standards and *E. coli* total lipid extracts were purchased from Avanti Polar Lipids, Inc. (Alabaster). 3-(2,2,6,6-Tetramethylpiperidin-1-yloxymethyl)-picolinic acid 2,5-dioxopyrrolidin-1-yl ester (TPN) and 5-(2,2,6,6-tetramethylpiperidin-1-yloxymethyl) nicotinic acid 2,5-dioxopyrrolidin-1-yl ester (TBN) were synthesized in-house following a revised procedure.[35,36] Details for the synthesis are described in the Supporting Information. Phospholipase $A_2$ ($PLA_2$) from *Crotalus adamanteus* venom was purchased from Aladdin. *B. subtilis* strain 168 was obtained from American Type Culture Collection (ATCC). All chemical reagents and organic solvents were purchased commercially (Supporting Information).

**Derivatization of PE with TPN/TBN.** Dried lipid standards (10 μM) and lipid extracts (~100 μM) were redissolved in acetonitrile (ACN) (260 μL) and added with triethylammonium bicarbonate (TEAB, 30 μL) and TPN/TBN (0.02 M, 60 μL) freshly prepared in $CH_2Cl_2$/DMF (1:1, v/v). The reaction solution was vortexed at 50 °C for 60 min, then mixed with 150 μL of MeOH for a subsequent reversed-phase liquid chromatography (RPLC)-MS analysis. No obvious degradation of PE was found from heating at 50 °C for 60 min as monitored by neutral loss scan (NLS) 141 Da of the protonated PE species.

**Bacteria Culture and Lipid Extraction.** *B. subtilis* cells were cultured in Luria−Bertani Broth (Solarbio) on an orbital


https://doi.org/10.1021/jasms.2c00011
J. Am. Soc. Mass Spectrom. 2022, 33, 714−721

shaker (250 rpm) at a constant temperature of 37 °C for 24 h. Lipids were extracted from 1 × $10^{10}$ harvested cells according to a modified Folch method[38] and finally dissolved in MeOH. Details of the lipid extraction are provided in the Supporting Information.

**$PLA_2$ Digestion.** *B. subtilis* lipid extracts were hydrolyzed by $PLA_2$ following a previously published protocol.[39] Briefly, lipid extracts (1 mL) were dried and dissolved in diethyl ether−methanol (99:1, v/v, 800 μL), and to this solution was added an aqueous solution (450 μL) containing 20 mM Tris-HCl, 40 mM calcium chloride, and 8 μg of $PLA_2$. The mixture was vigorously vortexed at room temperature for 5 h. The resulting hydrolyzed lipids were extracted and derivatized with the TPN reagent.

**RPLC-MS.** RPLC-MS experiments were performed on a QTRAP 4500 mass spectrometer (Sciex) hyphenated with a 20AD HPLC system (Shimadzu). The injection volume was 2 μL per run. The mobile phase consisted of A: ACN/$H_2O$ (60/40, v/v, 20 mM ammonium formate), and B: ACN/IPA (10/90, v/v, 0.2% formic acid). The gradient elution was applied at a flow rate of 0.26 mL/min through a C18 column (150 mm × 3 mm, 2.7 μm; Sigma-Aldrich) at 55 °C. The optimized gradients for TPN-derivatized PE and LPE are provided in the Supporting Information. The MS parameters were set as follows: ESI voltage, ±4500 V; curtain gas, 30 psi; interface heater temperature, 450 °C; ion source gas 1 and gas 2, 30 psi; declustering potential, ±100 V; CID energy, ±35−50 eV.

## RESULTS AND DISCUSSION

**Characterization of Cyclopropane Modification and C=C in PE.** TBN and TPN were both used for derivatizing PE and LPE (Scheme S1, Supporting Information). The concentration of TBN/TPN was kept above 2 mM, in large excess relative to that of the lipid standard (10 μM) or lipid extracts (~100 μM). Under the optimized conditions an almost quantitative conversion was achieved for the derivatization of PE standards from each reagent (Figure S2, Supporting Information). TBN and TPN share a common radical precursor group, namely, 2,2,6,6-tetramethylpiperidine-1-oxy (TEMPO). The only difference is that TBN consists of a phenyl, while TPN has a pyridine functional group. Upon low-energy CID the nitroxyl bond in TEMPO undergoes homolytic cleavage at high efficiency resulting from its low bond dissociation energy (BDE, ~125.5 kJ/mol)[40] and the high thermal stability of the TEMPO radical (Scheme 1). The resulting benzyl radical or pyridine methyl radical have similar C−H BDEs around 376.6 kJ/mol. However, as shown by Gao et al. the pyridine has a high proton affinity and thus can effectively reduce charge-directed fragmentation and promote RDD in positive ion mode.[36] A synthetic standard, PE 16:0/17:1(*cn*-7), was used to evaluate the gas-phase fragmentation behavior under CID. Figure 1a,b compares the $MS^2$ CID data ($m/z$ 500−1000) of the TPN-derivatized PE 16:0/17:1(*cn*-7) in positive-ion ($[M^{TPN}+H]^+$, $m/z$ 978.6) and negative-ion ($[M^{TPN}-H]^-$, $m/z$ 976.6) modes, respectively. The full-range mass spectra ($m/z$ 100−1000) are provided in Figure S3, Supporting Information. It is evident that, upon CID, homolytic cleavage of the labile nitroxyl bond is the dominant fragmentation channel, yielding the carbon-centered radical precursor ions, specifically, $m/z$ 822.5 in Figure 1a and $m/z$ 820.6 in Figure 1b, due to the neutral loss of the TEMPO moiety (156 Da). The resulting structures of the radical ions are shown in the insets of Figure 1. The C−H BDE in the

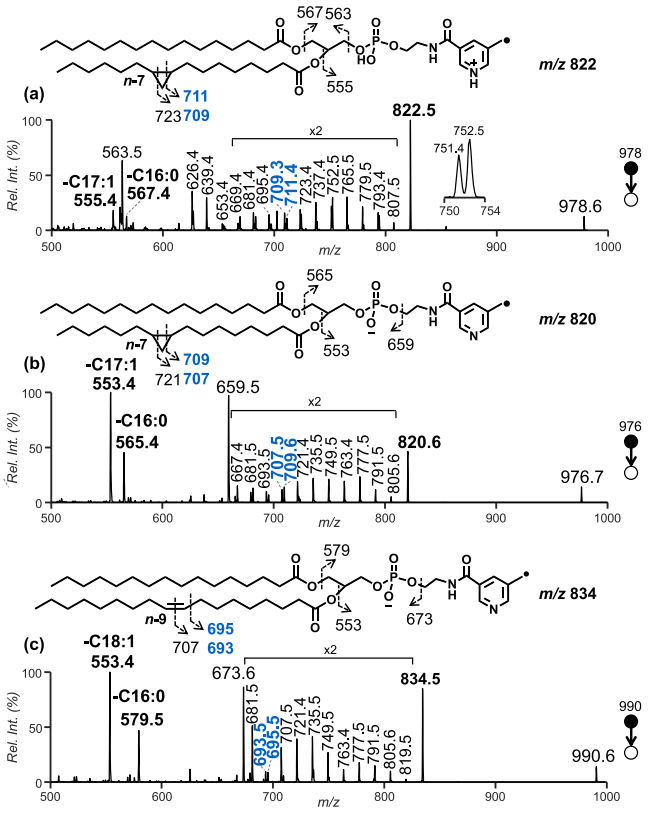


**Figure 1.** (a) $MS^2$ CID of TPN-derivatized PE 16:0/17:1(*cn*-7) ($[M^{TPN}+H]^+$, $m/z$ 978.6) in positive-ion mode. $MS^2$ CID of (b) TPN-derivatized PE 16:0/17:1(*cn*-7) ($[M^{TPN}-H]^-$, $m/z$ 976.7) and (c) PE 16:0/18:1(*n*-9) ($[M^{TPN}-H]^-$, $m/z$ 990.6) in negative-ion mode.

methyl group of 3-methylpyridine is ~376.6 kJ/mol, while that of the aliphatic C−H bonds is typically less than 410 kJ/mol.[40,41] Given that CID can provide the radical precursor ion with extra internal energy, it can readily abstract a hydrogen atom from the fatty acyl chain and trigger RDD. Subsequent RDD leads to rich fragmentations that are absent in $MS^2$ CID mass spectra obtained from the underivatized lipid (Figure S4, Supporting Information). For instance, an array of product ions with a 14 Da mass spacing is observed, that is, $m/z$ 807.5, 793.4, 779.5, 765.5, 751.4 (Figure 1a) or $m/z$ 805.6, 791.5, 777.5, 763.4, 749.5 (Figure 1b). These product ions can be rationalized as consecutive homolytic cleavage of unmodified C−C bonds along the fatty acyl chain. Both even- and odd-electron fragments are present among these product ions, which can be attributed to the losses of alkyl radicals or alkenes from the lipid radical ion, respectively. For example, $m/z$ 751.4 in Figure 1a is an even-electron product ion generated via a loss of $\cdot C_5H_{11}$, while the odd-electron ion at $m/z$ 752.5 is derived from a loss of $C_5H_{12}$ (inset of Figure 1a). Except for this pair of ions in which the odd-electron ion ($m/z$ 752.5) is of slightly higher ion abundance, the even-electron product ions are found to have higher ion abundances relative to the odd-electron fragment ions, probably due to higher stability.

As highlighted in blue font in Figure 1, the doublet with 2 Da mass difference corresponds to cross-ring C−C cleavage on the cyclopropane moiety. These ions ($m/z$ 711.4 and 709.3, positive-ion mode; $m/z$ 709.6 and 707.5, negative-ion mode) cause an interruption to the 14 Da spacing pattern for an unmodified fatty acyl chain and thus can be used as a signature


https://doi.org/10.1021/jasms.2c00011
J. Am. Soc. Mass Spectrom. 2022, 33, 714−721

for locating the cyclopropane modification between the *n*-7 and *n*-8 positions in this lipid.

The above RDD approach was also tested for locating C=C in PE 16:0/18:1(*n*-9). As displayed in Figure 1c, the $MS^2$ CID of the TPN-derivatized lipid ions ($[M^{TPN}-H]^-$, *m/z* 990.6) gives rise to a doublet at *m/z* 695.5 and 693.5, in which a spectral "gap" due to the drastically reduced ion abundances relative to adjacent fragment ions is distinct from a C=C moiety. A similar spectral gap has been previously reported for fragmentation adjacent to a C=C by RDD via $HCO_3^-$,[33] EIEIO,[22] or ion/ion chemistry.[42] However, it is difficult to use the RDD method for locating C=C bonds in a polyunsaturated chain due to the absence of gap signatures (data provided in Figure S5, Supporting Information). It is important to emphasize that RDD for cyclopropane does not render a spectral gap, permitting a certain degree of differentiation between cyclopropane and C=C in monounsaturated PE lipids.[26] $MS^3$ CID of the radical precursor ions shows similar fragmentation pattern as those shown in Figure 1, supporting the notion that the above-mentioned fragments are indeed caused by RDD (Figure S3c, Supporting Information).

Besides intrachain fragmentation, product ions resulting from the neutral losses of the fatty acyls such as $CO_2$ and R·[32,43] from the lipid radical ion via HAT from C1, C2, or C3 on the glycerol backbone are also observed (Scheme 1 and Scheme S2), providing direct evidence of the fatty acyl chain information. These ions include *m/z* 555.4, 567.4 (Figure 1a, positive ion) and *m/z* 553.4, 565.4 (Figure 1b, negative ion) for PE 16:0/17:1(c*n*-7), and *m/z* 555.2, 581.3 (Figure S6, Supporting Information, positive ion) and *m/z* 553.4, 579.5 (Figure 1c, negative ion) for PE 16:0/18:1(*n*-9). There is no obvious *sn*-specificity for this type of losses, likely due to a lack of preference of HAT from the glycerol backbone to the pyridine methyl radical. In addition, the fragment ions due to a loss of the modified headgroup are observed at *m/z* 563.5 in positive-ion mode (Figure 1a) and *m/z* 659.5 in negative-ion mode (Figure 1b), which are likely driven from charge-directed fragmentation.

TBN-derivatized PEs were subjected to $MS^2$ CID to evaluate the performance of RDD for localizing cyclopropane and C=C. In the negative-ion mode, the fragmentation pattern is similar to that described for TPN-derivatized PEs (Figure S7a,c, Supporting Information). This is likely due to the similar reactivity of the radical precursor ions from the two reagents. Note that the C–H BDE in the methyl group of methylbenzene is 370.3 kJ/mol.[40] As a contrast, little RDD is observed from $MS^2$ CID in the positive-ion mode because of protonation at the TEMPO moiety (Figure S7b, Supporting Information).[36]

The limit of identification (LOI, signal-to-noise ratio (S/N) > 3) for PE 16:0/17:1(c*n*-7) and PE 16:0/18:1(*n*-7) was achieved at 25 nM with a 2 μL injection from TPN or TBN derivatization in the negative-ion mode. As demonstrated above, TPN can be used in either positive-ion or negative-ion mode to induce RDD, while TBN can only be used with negative-ion mode. Therefore, TPN was chosen for further studies. Considering that the product ions indicative of acyl substituents were much more abundant in negative-ion mode, further studies for a structural characterization of PE containing C=C or cyclopropane were performed in negative-ion mode.

**Structural Characterization of Methyl Branching in PE.** Because of a lack of PE standards containing monomethyl branched chain, PE 4Me-16:0/4Me-16:0 was used as a representative example to demonstrate the capability of TPN-based RDD for characterization of the methyl branching in a fatty acyl chain. In this lipid, there are four methyl branching points in each fatty acyl chain, located at the *n*-2, *n*-6, *n*-10, and *n*-14 positions. The $MS^2$ CID of TPN derivatized lipid ions in positive-ion mode results in an abundant formation of the carbon-centered radical precursor ions at *m/z* 922.6 as well as rich intrachain cleavages from RDD (Figure 2a). These product ions arise from a major (blue) and

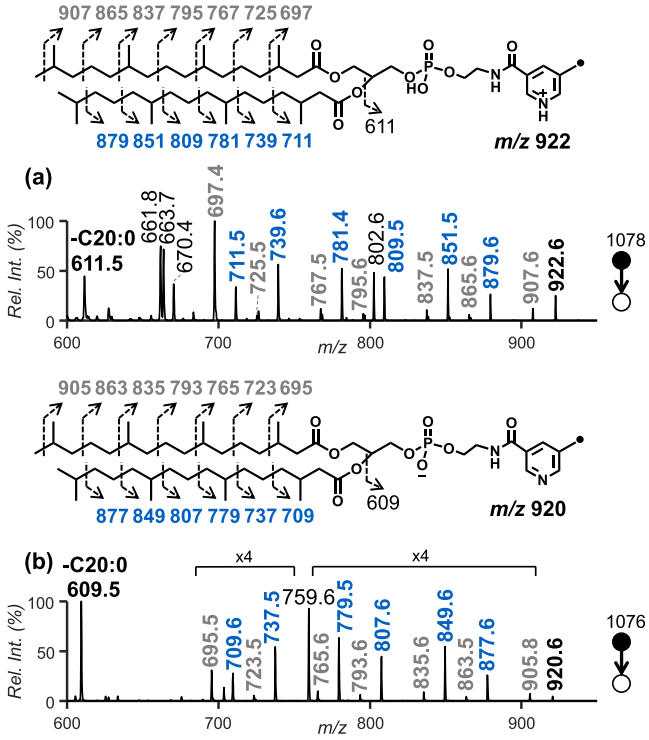


**Figure 2.** $MS^2$ CID of TPN-derivatized PE 4Me-16:0/4Me-16:0 in (a) positive-ion mode ($[M^{TPN}+H]^+$, *m/z* 1078.6) and (b) in negative-ion mode ($[M^{TPN}-H]^-$, *m/z* 1076.6).

a minor (gray) dissociation pathway, respectively (Scheme S3). In the major dissociation pathway, the nascent radical precursor ion favors HAT from the tertiary carbon at the methyl branching or the secondary carbon at the β-position to the branching point. Subsequent α-cleavage to the tertiary-carbon radicals gives rise to product ions at *m/z* 851, 781, 711 and *m/z* 879, 809, 739. The similar fragmentation pathways were previously observed for RDD induced via $MS^2$ CID of $HCO_3^-$ adducts of LPC[33] and SM[34] or RDD initiated by UVPD of the C–I bond.[31] The minor dissociation pathway involves the formation of radicals at the α-position to the methyl branching, leading to product ions at *m/z* 907, 837, 767, 697 and *m/z* 865, 795, 725. Note that the ion at *m/z* 697 ion is of high abundance, probably driven by the stability of the radical formed at the α-position of the carbonyl carbon. The appearance of ions at *m/z* 670, an odd-electron product ion, can be explained by the same reason. Overall, the 14 Da spacing between peaks is interrupted by a 28 Da spacing, for example, between the product ions at *m/z* 837 and 809, providing a diagnosis of the presence and location of methyl branching. The distinct fragmentation pattern clearly distinguishes it from a straight-chain PE (Figure S8, Supporting


https://doi.org/10.1021/jasms.2c00011
J. Am. Soc. Mass Spectrom. 2022, 33, 714–721

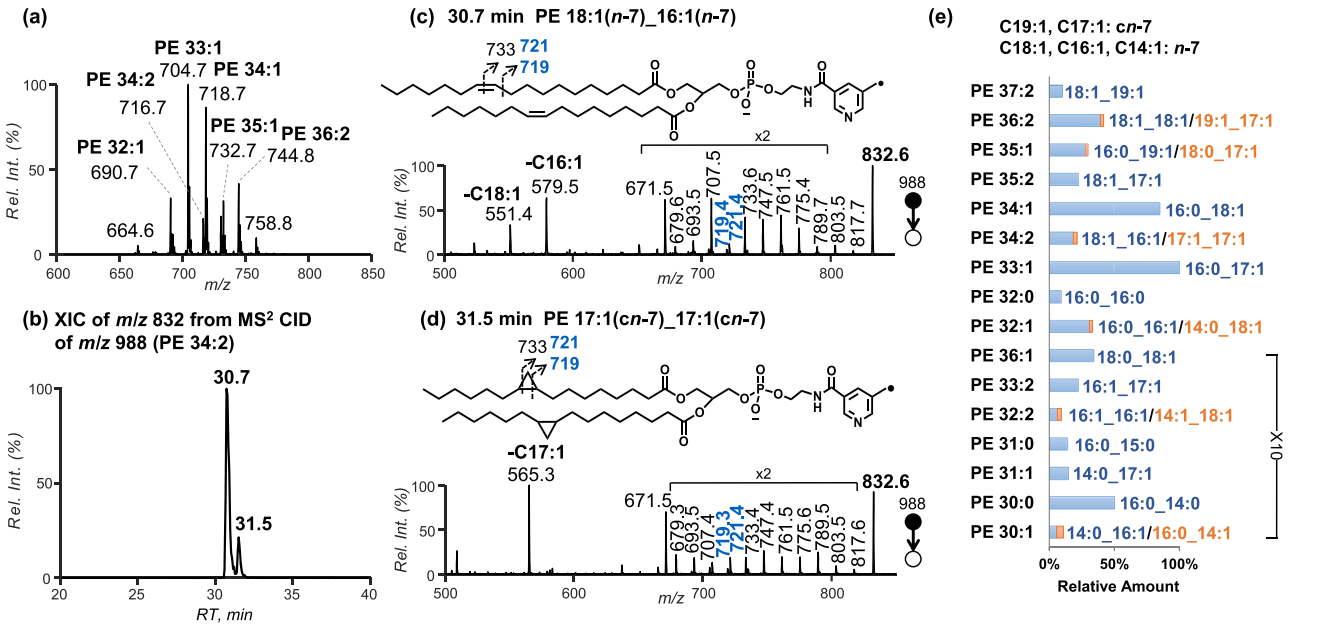


**Figure 3.** (a) The PE profile of *E. coli* via NLS of 141 Da in positive-ion mode. (b) XIC of $m/z$ 832 from $MS^2$ CID of $[PE^{TPN}$ 34:2 -H$]^-$ ($m/z$ 988) and the corresponding spectra for the peaks eluted at (c) 30.7 and (d) 31.5 min, respectively. (e) Identified PEs from *E. coli* with relative ion abundances normalized to PE 33:1. The locations of C═C and cyclopropane in fatty acyls are indicated at the top of (e).

Information). The $MS^2$ CID results of the derivatized lipid in the negative-ion mode (Figure 2b) are in accordance with those of the positive-ion mode, albeit with a relatively lower abundance of product ions detected. The fragments at $m/z$ 611.5 (Figure 2a) and $m/z$ 609.5 (Figure 2b) are derived from the loss of fatty acyl as $CO_2$ and R· from the lipid radical ion. As for LPE, besides intrachain fragmentation from the methyl tail, positive-ion RDD promotes rearrangement within headgroup moiety, which complicates mass spectra. Therefore, RDD in the negative-ion mode was chosen for the analysis of LPEs from bacteria lipid samples.

**Identification of PEs from Lipid Extracts of E. coli.** The outlined approach was applied to the structural identification of PEs in *E. coli*. Figure 3a shows the NLS of 141 Da (the phosphoethanolamine headgroup) from underivatized lipid extracts of *E. coli*. The most abundant PE species is PE 33:1, followed by PE 34:1, PE 36:2, PE 32:1, and PE 35:1. The TPN-derivatized sample was then subjected to RPLC-MS/MS analyses, in which TPN-derivatized PE species eluted between 27 and 35 min (Figure S9a, Supporting Information). NLS of 141 Da was performed to detect the remaining PE lipids, and we confirmed that the derivatization was complete (Figure S9b, Supporting Information). The PE profile of *E. coli* can also be obtained via NLS of 156 Da, the neutral loss of TEMPO from TPN derivatized sample, although less sensitive than NLS of 141 Da (Figures S9c and 8d, Supporting Information). $MS^2$ CID in negative-ion mode reveals that the TPN-derivatized PE 33:1 ($m/z$ 976.6), the most abundant PE species, contains a cyclopropane motif, according to the appearance of a doublet at $m/z$ 709.4/707.5 without showing a significant gap in the spectrum (Figure S10a, Supporting Information). Together with the product ions observed at $m/z$ 553.4 and 565.6, which are indicative of the loss of C17:1 and C16:0, respectively, this PE lipid is identified as PE 16:0_17:1(*cn*-7).

The extracted-ion chromatogram (XIC) of TPN-derivatized PE 34:2 ($m/z$ 988, Figure 3b) suggests the presence of two structural isomers eluted at 30.7 min (86%) and 31.5 min (14%), respectively. The major peak is identified as PE 18:1_16:1 based on the detection of fatty acyl-related ions at $m/z$ 551.4 (-C18:1) and 579.5 (-C16:1). In addition, the spectral gap at $m/z$ 721.4 and 719.4 confirms a C═C at *n*-7 position (Figure 3c). Thus, it is identified as PE 18:1(*n*-7)_16:1(*n*-7). For the minor peak, a cyclopropane ring at the *n*-7 position is determined in 17:1 fatty acyl (Figure 3d). Therefore, this lipid is identified as PE 17:1(*cn*-7)_17:1(*cn*-7). Such analyses have the advantage of assigning the fatty acyl constituents and the location of C═C or cyclopropane moiety from one single RDD spectrum. Examples for the identification of other PE species are provided in Figures S10 and S11, Supporting Information.

In total, 22 PE molecular species are identified (Figure 3e, Table S1), including 6 cyclopropyl PE, 10 unsaturated PE, and 3 PE containing both cyclopropane and C═C, consistent with previous reports using UVPD.[23,25,44] It is worth noting that the presented approach cannot provide the definite structures for PE species containing both C═C and cyclopropane moieties because of the need to use a spectral gap to differentiate the two. Therefore, the locations of C═C and cyclopropane were separately confirmed via PB-$MS^3$ CID and RDD after $PLA_2$ hydrolysis, respectively (Figure S12, Supporting Information). Notably, all identified cyclopropane rings are localized to the *n*-7 position within C17:1 and C19:1, and all positions of C═C occur at the *n*-7 position within C16:1 and C18:1. This result corroborates that the cyclopropane rings in C17:1 and C19:1 are generated from in situ methylenation of the C═C bonds in C16:1 and C18:1 via the catalysis of cyclopropane synthase.[4]

**Identification of LPEs from B. subtilis Lipid Extracts.** As intrachain cleavages induced by RDD occur in both fatty acyl chains of PE, an unambiguous assignment of methyl branching to a specific acyl chain is challenging. To circumvent this issue, $PLA_2$ hydrolysis was performed to remove the *sn*-2 fatty acyl of PEs and convert them into LPEs for further analysis. The lipid extracts from *B. subtilis* strain 168 were


https://doi.org/10.1021/jasms.2c00011
J. Am. Soc. Mass Spectrom. 2022, 33, 714−721

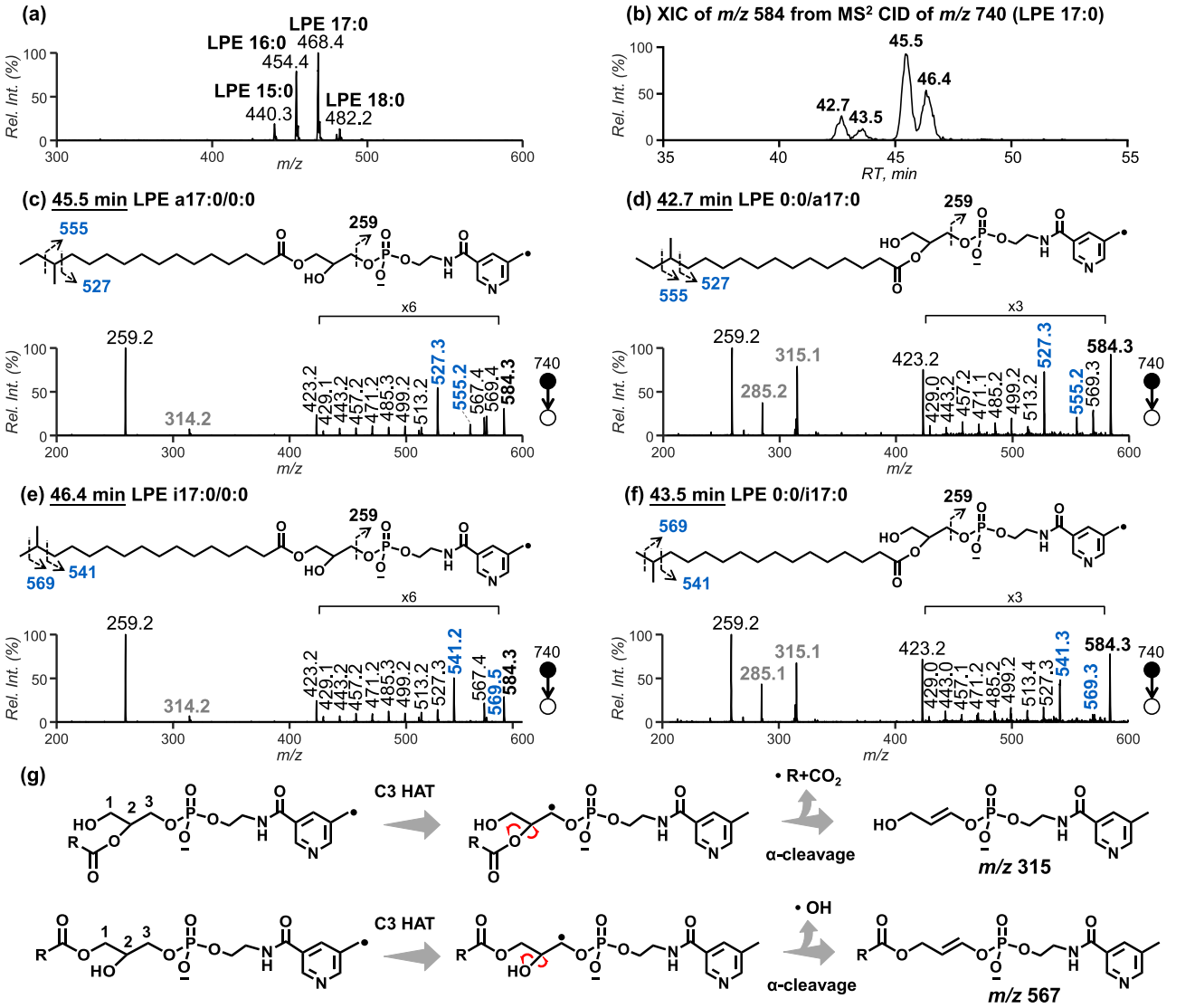


**Figure 4.** (a) The profile of LPEs via NLS of 141 Da from *B. subtilis* after $PLA_2$ hydrolysis. (b) XIC of *m/z* 584 from $MS^2$ CID of $[LPE^{TPN}$ 17:0 -H$]^-$ (*m/z* 740) and the mass spectra of the peaks eluted at (c) 45.5, (d) 42.7, (e) 46.4, and (f) 43.5 min. (g) Proposed RDD accounting for *sn*-2 (top) and *sn*-1 (bottom) specific fragmentation.

treated with $PLA_2$ and then analyzed. The $MS^1$ profile of PEs before hydrolysis (Figure S13, Supporting Information) and LPEs after hydrolysis (Figure 4a) reveal that *B. subtilis* are enriched in saturated PE species. After the hydrolysis, LPE 17:0 is the most abundant species, followed by LPE 16:0, LPE 15:0, and LPE 18:0 (Figure 4a).

Figure 4b shows the XIC of *m/z* 584 (−156 Da) from $MS^2$ CID of $[LPE^{TPN}$ 17:0 -H$]^-$ (*m/z* 740). Four peaks are well-separated at 42.7, 43.5, 45.5, and 46.4 min, respectively. The peak eluted at 45.5 min (Figure 4c) is identified as LPE a17:0/0:0 based on the observation of a 28 Da gap between product ions at *m/z* 555.2 and 527.3, while the peak at 46.4 min is determined as LPE i17:0/0:0, according to a 28 Da gap between product ions at *m/z* 569.5 and 541.2 (Figure 4e). Another two peaks, eluted at 42.7 and 43.5 min, are the *sn*-2 isomers, that is, LPE 0:0/a17:0 and LPE 0:0/i17:0 (Figure 4d,f). These *sn*-isomers are likely formed during or after $PLA_2$, resulting from acyl transfer reactions in solution.[45] We note that RDD of the *sn*-1 isomers generates a weak fragment peak at *m/z* 314.2 via neutral loss of the fatty acid, while the peak at *m/z* 315.1 corresponding to loss of the fatty acyl as $CO_2$ and R· is dominant for the *sn*-2 isomers. A possible fragmentation pathway for the selective loss of $CO_2$ and R· for *sn*-2 LPE is proposed in Figure 4g, in which HAT from C3 is considered to be more preferable than that from C1. On the one hand, the peak at *m/z* 285.2 is also abundant for the *sn*-2 isomers, which might be derived from the loss of $CH_2O$ from *m/z* 315.1. On the other hand, the fragment peak at *m/z* 567.4, arising from loss of OH· from the radical precursor ion, is much more abundant for the *sn*-1 isomers than that of the *sn*-2 isomers likely also due to a more favorable HAT from C3 to the pyridine methyl radical (Figure 4g). Thus, these spectral characteristics afford a confident assignment of *sn*-isomers of LPE. A common fragment peak at *m/z* 259.2 is observed for both *sn*-isomers, corresponding to the modified headgroup, which is useful for the identification of a PE headgroup. Similarly, LPE a15:0/0:0 and LPE i15:0/0:0 as well as their *sn*-2 isomers are identified (Figure S14, Supporting Information).

LPE 16:0 is identified to be a mixture of LPE 16:0/0:0 (major component) and LPE i16:0/0:0 (minor component), while LPE 18:0/0:0 only contains the straight chain. In total, 14 LPEs are identified from *B. subtilis* lipid extracts hydrolyzed


https://doi.org/10.1021/jasms.2c00011
J. Am. Soc. Mass Spectrom. 2022, 33, 714−721

by PLA2 (Table S2, Supporting Information). Among them, six LPEs contain iso-methyl branching, while four LPEs contain anteiso-methyl branching. The results are consistent with those of a previous report using gas chromatography (GC)-MS for the analysis of total fatty acids.[46] Compared to GC-MS, the presented approach has the advantages of analyzing intact LPE species and independent identification without relying on standards.

## CONCLUSIONS

We have developed an RDD approach that can be initiated by low-energy CID for a detailed structural characterization of intrachain modifications within PEs and LPEs. Abundant lipid radical ions are generated via a homolytic cleavage of the nitroxyl bond in the TEMPO moiety. The spectral features derived from RDD enable identification of C=C, cyclopropane ring, and isomeric *iso*- and *anteiso*-methyl branching as well as the *sn*-isomers of LPE. The LOI (S/N > 3) for PE 16:0/17:1(*cn*-7) and PE 16:0/18:1(*n*-7) standard can be achieved at 25 nM by using either TPN or TBN derivatization reagent in negative-ion mode. As demonstrated with the analysis of *E. coli* lipid extracts, the above RDD approach allows one to identify 22 PE lipid species, including 19 PE containing cyclopropane and/or C=C that cannot be resolved via conventional CID. In addition, LPEs obtained from $PLA_2$ hydrolyzed *B. subtilis* lipid extract were characterized with *iso*- or *anteiso*-methyl branching or a straight acyl chain. The developed approach is more sensitive in the aspect of characterizing chain modifications, as compared to RDD via $HCO_3^-$, where limited RDD channels occur within fatty acyls. Moreover, this approach confers a high efficiency in forming lipid radical ions via CID, without the need of an instrument modification that is required for UVPD of the C−I bond. The major limitation for the current approach is that it can only be used for the analysis of amino-containing lipids, for example, PEs and LPEs, because the radical initiator is conjugated onto amine functional groups. In a future study, the scope will be expanded to other amino-containing lipids, for example, sphingosine and phosphoserine, and novel radical precursors will be designed for other lipid classes.

## ASSOCIATED CONTENT

### Supporting Information

The Supporting Information is available free of charge at https://pubs.acs.org/doi/10.1021/jasms.2c00011.

Materials, lipid extraction, synthesis of TPN and TBN, LC separation conditions, structural characterization of cyclopropane, C=C and methyl branching in PE fatty acyl chain, identification of PEs from *E. coli* lipid extracts, and identification of LPEs from *Bacillus subtilis* lipid extracts (PDF)

## AUTHOR INFORMATION


### Corresponding Author

**Yu Xia** − *Department of Chemistry, MOE Key Laboratory of Bioorganic Phosphorus Chemistry & Chemical Biology, Tsinghua University, Beijing 10084, China;* orcid.org/0000-0001-8694-9900; Email: xiayu@mail.tsinghua.edu.cn

### Authors

**Qiaohong Lin** − *Department of Chemistry, MOE Key Laboratory of Bioorganic Phosphorus Chemistry & Chemical Biology, Tsinghua University, Beijing 10084, China*

**Pengyun Li** − *National Engineering Research Center for the Emergency Drug, Beijing Institute of Pharmacology and Toxicology, Beijing 100850, China*

**Ruijun Jian** − *Department of Chemistry, MOE Key Laboratory of Bioorganic Phosphorus Chemistry & Chemical Biology, Tsinghua University, Beijing 10084, China*

Complete contact information is available at: https://pubs.acs.org/10.1021/jasms.2c00011


### Author Contributions

Y.X. initiated the project. Q.L. and Y.X. designed the experiments. Q.L. performed the research. P.L. synthesized the derivatization reagents and prepared the bacterial samples. Q.L. and R.J. analyzed the data. Q.L. and Y.X. cowrote the paper. All authors discussed the results and commented on the paper.

### Notes

The authors declare no competing financial interest.

## ACKNOWLEDGMENTS

Financial support from the National Key R&D Program of China (2018YFA0800903) and National Natural Science Foundation of China (No. 22074075) is greatly appreciated.

## REFERENCES


(1) Zhang, Y.; Rock, C. O. Membrane lipid homeostasis in bacteria. *Nat. Rev. Microbiol.* **2008**, *6*, 222−233.

(2) Diomandé, S. E.; Nguyen-The, C.; Guinebretière, M.-H.; Broussolle, V.; Brillard, J. Role of fatty acids in Bacillus environmental adaptation. *Front. Microbiol.* **2015**, *6*, 813−813.

(3) Poger, D.; Mark, A. E. A ring to rule them all: the effect of cyclopropane fatty acids on the fluidity of lipid bilayers. *J. Phys. Chem. B* **2015**, *119*, 5487−5495.

(4) Grogan, D. W.; Cronan, J. E., Jr. Cyclopropane ring formation in membrane lipids of bacteria. *Microbiol. Mol. Biol. Rev.* **1997**, *61*, 429−441.

(5) Takayama, K.; Wang, C.; Besra, G. S. Pathway to synthesis and processing of mycolic acids in Mycobacterium tuberculosis. *Clin. Microbiol. Rev.* **2005**, *18*, 81−101.

(6) Kaneda, T. Iso- and anteiso-fatty acids in bacteria: biosynthesis, function, and taxonomic significance. *Microbiol. Rev.* **1991**, *55*, 288−302.

(7) Wallace, M.; Green, C. R.; Roberts, L. S.; Lee, Y. M.; McCarville, J. L.; Sanchez-Gurmaches, J.; Meurs, N.; Gengatharan, J. M.; Hover, J. D.; Phillips, S. A.; Ciaraldi, T. P.; Guertin, D. A.; Cabrales, P.; Ayres, J. S.; Nomura, D. K.; Loomba, R.; Metallo, C. M. Enzyme promiscuity drives branched-chain fatty acid synthesis in adipose tissues. *Nat. Chem. Biol.* **2018**, *14*, 1021−1031.

(8) Ran-Ressler, R. R.; Devapatla, S.; Lawrence, P.; Brenna, J. T. Branched chain fatty acids are constituents of the normal healthy newborn gastrointestinal tract. *Pediatr. Res.* **2008**, *64*, 605−609.

(9) Tanno, H.; Sassa, T.; Sawai, M.; Kihara, A. Production of branched-chain very-long-chain fatty acids by fatty acid elongases and their tissue distribution in mammals. *Biochim. Biophys. Acta, Mol. Cell. Biol. Lipids* **2021**, *1866*, 158842.

(10) Siliakus, M. F.; van der Oost, J.; Kengen, S. W. M. Adaptations of archaeal and bacterial membranes to variations in temperature, pH and pressure. *Extremophiles* **2017**, *21*, 651−670.

(11) Porta Siegel, T.; Ekroos, K.; Ellis, S. R. Reshaping Lipid Biochemistry by Pushing Barriers in Structural Lipidomics. *Angew. Chem., Int. Ed.* **2019**, *58*, 6492−6501.

(12) Rustam, Y. H.; Reid, G. E. Analytical challenges and recent advances in mass spectrometry based lipidomics. *Anal. Chem.* **2018**, *90*, 374−397.
(13) Wang, J.; Wang, C.; Han, X. Tutorial on lipidomics. *Anal. Chim. Acta* **2019**, *1061*, 28−41.
(14) Murphy, R. C. In *Tandem Mass Spectrometry of Lipids: Molecular Analysis of Complex Lipids;* Royal Society of Chemistry, 2015.
(15) Ma, X.; Xia, Y. Pinpointing double bonds in lipids by Paternò-Büchi reactions and mass spectrometry. *Angew. Chem., Int. Ed.* **2014**, *53*, 2592−2596.
(16) Ma, X.; Chong, L.; Tian, R.; Shi, R.; Hu, T. Y.; Ouyang, Z.; Xia, Y. Identification and quantitation of lipid C=C location isomers: A shotgun lipidomics approach enabled by photochemical reaction. *Proc. Natl. Acad. Sci. U.S.A.* **2016**, *113*, 2573−2578.
(17) Kuo, T.; Chung, H.; Chang, H.; Lin, C.; Wang, M.; Shen, T.; Hsu, C. Deep lipidomics and molecular imaging of unsaturated lipid isomers: a universal strategy initiated by mCPBA epoxidation. *Anal. Chem.* **2019**, *91*, 11905−11915.
(18) Zhang, H.; Xu, M.; Shi, X.; Liu, Y.; Li, Z.; Jagodinsky, J. C.; Ma, M.; Welham, N. V.; Morris, Z. S.; Li, L. Quantification and molecular imaging of fatty acid isomers from complex biological samples by mass spectrometry. *Chem. Sci.* **2021**, *12*, 8115−8122.
(19) Unsihuay, D.; Su, P.; Hu, H.; Qiu, J.; Kuang, S.; Li, Y.; Sun, X.; Dey, S. K.; Laskin, J. Imaging and analysis of isomeric unsaturated lipids through online photochemical derivatization of carbon-carbon double bonds. *Angew. Chem., Int. Ed.* **2021**, *60*, 7559−7563.
(20) Pham, H. T.; Maccarone, A. T.; Thomas, M. C.; Campbell, J. L.; Mitchell, T. W.; Blanksby, S. J. Structural characterization of glycerophospholipids by combinations of ozone- and collision-induced dissociation mass spectrometry: the next step towards "top-down" lipidomics. *Analyst* **2014**, *139*, 204−214.
(21) Marshall, D. L.; Criscuolo, A.; Young, R. S. E.; Poad, B. L. J.; Zeller, M.; Reid, G. E.; Mitchell, T. W.; Blanksby, S. J. Mapping unsaturation in human plasma lipids by data-independent ozone-induced dissociation. *J. Am. Soc. Mass. Spectrom.* **2019**, *30*, 1621−1630.
(22) Campbell, J. L.; Baba, T. Near-complete structural characterization of phosphatidylcholines using electron impact excitation of ions from organics. *Anal. Chem.* **2015**, *87*, 5837−5845.
(23) Williams, P. E.; Klein, D. R.; Greer, S. M.; Brodbelt, J. S. Pinpointing double bond and sn-positions in glycerophospholipids via hybrid 193 nm ultraviolet photodissociation (UVPD) mass spectrometry. *J. Am. Chem. Soc.* **2017**, *139*, 15681−15690.
(24) Blevins, M.; James, V.; Herrera, C.; Purcell, A.; Trent, M. S.; Brodbelt, J. S. Unsaturation elements and other modifications of phospholipids in bacteria new insight from UVPD mass spectrometry. *Anal. Chem.* **2020**, *92*, 9146−9155.
(25) Blevins, M. S.; Klein, D. R.; Brodbelt, J. S. Localization of cyclopropane modifications in bacterial lipids via 213 nm ultraviolet photodissociation mass spectrometry. *Anal. Chem.* **2019**, *91*, 6820−6828.
(26) Randolph, C. E.; Shenault, D. S. M.; Blanksby, S. J.; McLuckey, S. A. Localization of Carbon-Carbon Double Bond and Cyclopropane Sites in Cardiolipins via Gas-Phase Charge Inversion Reactions. *J. Am. Soc. Mass. Spectrom.* **2021**, *32*, 455−464.
(27) Pham, H. T.; Trevitt, A. J.; Mitchell, T. W.; Blanksby, S. J. Rapid differentiation of isomeric lipids by photodissociation mass spectrometry of fatty acid derivatives. *Rapid Commun. Mass Spectrom.* **2013**, *27*, 805−815.
(28) Narreddula, V. R.; Boase, N. R.; Ailuri, R.; Marshall, D. L.; Poad, B. L. J.; Kelso, M. J.; Trevitt, A. J.; Mitchell, T. W.; Blanksby, S. J. Introduction of a fixed-charge, photolabile derivative for enhanced structural elucidation of fatty acids. *Anal. Chem.* **2019**, *91*, 9901−9909.
(29) Narreddula, V. R.; Sadowski, P.; Boase, N. R. B.; Marshall, D. L.; Poad, B. L. J.; Trevitt, A. J.; Mitchell, T. W.; Blanksby, S. J. Structural elucidation of hydroxy fatty acids by photodissociation mass spectrometry with photolabile derivatives. *Rapid Commun. Mass Spectrom.* **2020**, *34*, No. e8741.
(30) Pham, H. T.; Julian, R. R. Mass shifting and radical delivery with crown ether attachment for separation and analysis of phosphatidylethanolamine lipids. *Anal. Chem.* **2014**, *86*, 3020−3027.
(31) Pham, H. T.; Ly, T.; Trevitt, A. J.; Mitchell, T. W.; Blanksby, S. J. Differentiation of complex lipid isomers by radical-directed dissociation mass spectrometry. *Anal. Chem.* **2012**, *84*, 7525−7532.
(32) Zhao, X.; Zhang, W.; Zhang, D.; Liu, X.; Cao, W.; Chen, Q.; Ouyang, Z.; Xia, Y. A lipidomic workflow capable of resolving sn- and C=C location isomers of phosphatidylcholines. *Chem. Sci.* **2019**, *10*, 10740−10748.
(33) Zhao, X.; Xia, Y. Characterization of fatty acyl modifications in phosphatidylcholines and lysophosphatidylcholines via radical-directed dissociation. *J. Am. Soc. Mass. Spectrom.* **2021**, *32*, 560−568.
(34) Zhao, X.; Wu, G.; Zhang, W.; Dong, M.; Xia, Y. Resolving modifications on sphingoid base and N-acyl chain of sphingomyelin lipids in complex lipid extracts. *Anal. Chem.* **2020**, *92*, 14775−14782.
(35) Lee, M.; Kang, M.; Moon, B.; Oh, H. B. Gas-phase peptide sequencing by TEMPO-mediated radical generation. *Analyst* **2009**, *134*, 1706−1712.
(36) Gaspar, K.; Fabijanczuk, K.; Otegui, T.; Acosta, J.; Gao, J. Development of novel free radical initiated peptide sequencing reagent: application to identification and characterization of peptides by mass spectrometry. *J. Am. Soc. Mass. Spectrom.* **2019**, *30*, 548−556.
(37) Liebisch, G.; Fahy, E.; Aoki, J.; Dennis, E. A.; Durand, T.; Ejsing, C.; Fedorova, M.; Feussner, I.; Griffiths, W. J.; Koefeler, H.; Merrill, A. H., Jr.; Murphy, R. C.; O'Donnell, V. B.; Oskolkova, O. V.; Subramaniam, S.; Wakelam, M.; Spener, F. Update on LIPID MAPS classification, nomenclature and shorthand notation for MS-derived lipid structures. *J. Lipid Res.* **2020**, *61*, 1539−1555.
(38) Folch, J.; Lees, M.; Stanley, G.H. S. A simple method for the isolation and purification of total lipides from animal tissues. *J. Biol. Chem.* **1957**, *226*, 497−509.
(39) Ekroos, K.; Ejsing, C. S.; Bahr, U.; Karas, M.; Simons, K.; Shevchenko, A. Charting molecular composition of phosphatidylcholines by fatty acid scanning and ion trap MS3 fragmentation. *J. Lipid Res.* **2003**, *44*, 2181−2192.
(40) Luo, Y. *Handbook of Bond Dissociation Energies in Organic Compounds;* CRC Press: Boca Raton, FL, 2002.
(41) Blanksby, S. J.; Ellison, G. B. Bond Dissociation Energies of Organic Molecules. *Acc. Chem. Res.* **2003**, *36*, 255−263.
(42) Randolph, C. E.; Blanksby, S. J.; McLuckey, S. A. Toward complete structure elucidation of glycerophospholipids in the gas phase through charge inversion ion/ion chemistry. *Anal. Chem.* **2020**, *92*, 1219−1227.
(43) Poad, B. L.; Kirk, B. B.; Hettiarachchi, P. I.; Trevitt, A. J.; Blanksby, S. J.; Clark, T. Direct detection of a persistent carbonyloxyl radical in the gas phase. *Angew. Chem., Int. Ed.* **2013**, *52*, 9301−9304.
(44) Klein, D. R.; Blevins, M. S.; Macias, L. A.; Douglass, M.; Trent, M. S.; Brodbelt, J. S. Localization of double bonds in bacterial glycerophospholipids using 193 nm ultraviolet photodissociation in the negative mode. *Anal. Chem.* **2020**, *92*, 5986−5993.
(45) Plueckthun, A.; Dennis, E. A. Acyl and phosphoryl migration in lysophospholipids: importance in phospholipid synthesis and phospholipase specificity. *Biochemistry* **1982**, *21*, 1743−1750.
(46) Nickels, J. D.; Chatterjee, S.; Mostofian, B.; Stanley, C. B.; Ohl, M.; Zolnierczuk, P.; Schulz, R.; Myles, D. A. A.; Standaert, R. F.; Elkins, J. G.; Cheng, X.; Katsaras, J. Bacillus subtilis lipid extract, a branched-chain fatty acid model membrane. *J. Phys. Chem. Lett.* **2017**, *8*, 4214−4217.


https://doi.org/10.1021/jasms.2c00011
*J. Am. Soc. Mass Spectrom.* 2022, 33, 714−721